REVIEW

Fruit softening and pectin disassembly: An overview of the nano-structural pectin modifications assessed by atomic force microscopy (AFM)

Candelas Paniagua[1], Sara Posé[1], Victor J. Morris[2], Andrew R. Kirby[2], Miguel A. Quesada[3] and José A. Mercado[1,*]

[1]*Instituto de Hortofruticultura Subtropical y Mediterránea "La Mayora" (IHSM-UMA-CSIC), Departamento de Biología Vegetal, Universidad de Málaga, 29071, Málaga, Spain*

[2]*Institute of Food Research, Norwich Research Park, Colney, Norwich NR4 7UA, UK*

[3]*Departamento de Biología Vegetal, Universidad de Málaga, 29071, Málaga, Spain*

Running title: *Nano-structural characterization of fruit pectins by AFM*

**For correspondence: E-mail: mercado@uma.es*

Abstract

- *Background* One of the main factors that reduce fruit quality leading to economically important losses is oversoftening. Textural changes during fruit ripening are mainly due to the dissolution of the middle lamella, the reduction of cell to cell adhesion, and the weakening of parenchyma cell walls as result of the action of cell wall modifying enzymes. Pectins, one major component of fruit cell walls, are extensively modified during ripening. These changes include solubilization, depolymerization and the loss of neutral side chains. Recent evidences in fruits with soft or crisp textures at ripening, strawberry and apple, suggest that pectin disassembly is a key factor in textural changes. In both fruits, softening was reduced as result of antisense down-regulation of polygalacturonase genes. Changes in pectic polymer size, composition and structure have traditionally been studied by conventional techniques, most of them relying on bulk analysis of a population of polysaccharides but studies focusing in the modifications at the nano-structural level are scarce. Atomic force microscopy allows the study of individual polymers at high magnification and with minimal sample preparation; however, AFM has scarcely been employed to analyze pectin disassembly during fruit ripening.
- *Scope* Firstly, the main features of the pectin disassembly process during fruit ripening are discussed. Then, the nano-structural characterization of fruit pectins by AFM and its relationship with texture and postharvest fruit shelf life is reviewed. In general, fruit pectins are visualized under AFM as linear chains, few of them showing long branches, and aggregates. Number- and weight-average values obtained from these images are in good agreement with chromatographic analyses. Most AFM studies indicate a reduction in the length of individual pectin chains and

in the frequency of aggregates as the fruit ripen, being pectins extracted with sodium carbonate, supposedly located within the primary cell wall, the most affected.

Key words: Atomic force microscopy, cell wall, fruit softening, fruit ripening, homogalacturonan, pectins, rhamnogalacturonan

INTRODUCTION

Ripening of fleshy fruit is one of the last developmental phases of fruit ontogeny involving many genetic, biochemical and physiological modifications. Among others, changes include the accumulation of pigments and sugars, the production of aromatic compounds and flesh softening (Gapper *et al.*, 2013). All these changes have evolved to make edible fruits more attractive to seed dispersal organisms. Ripening also enhances fruit organoleptic properties, making them adequate for human consumption. However, fruit quality diminishes as ripening reaches an advanced stage, mainly due to fruit oversoftening, increased pathogen susceptibility and the development of undesirable flavor and skin color, leading to important economic losses during postharvest fruit managing (Bapat *et al.*, 2010). Thus, the rate of fruit softening not only determines the postharvest shelf life but also other economically important aspects such as the frequency of harvest, the handling procedures or the distance that the fruits can be transported. Therefore, the delaying of fruit softening is one of the major targets for breeding programs in most commodities. Based on the degree of softening during ripening, fleshy fruits are classified into two categories (Bourne, 1979), those that soften greatly as they ripen, acquiring a melting texture and usually having a short postharvest life (e.g., strawberry, peach, apricot, tomato) and those that soften moderately as they

ripen, retain a crisp texture and have a long storage life (e.g., apple, pear, watermelon).

Firmness and juiciness are the most important textural components in the case of fleshy fruits (Toivonen and Brummell, 2008). Both features are largely determined by the characteristics of parenchyma cells (shape and size, cell wall thickness and strength, cell turgor) and the extension and strength of adhesion areas between adjacent cells (Harker *et al.*, 1997). During ripening, parenchyma cell walls are extensively modified, altering their mechanical properties, and cell adhesion is significantly reduced as result of middle lamella dissolution. Cell wall and middle lamella modifications leading to fruit softening result from the action of cell wall modifying enzymes (e.g., polygalacturonase (PG), pectin methyl esterase (PME), pectate lyase, β-galactosidase, cellulase) generally encoded by ripening-related genes (Brummell and Harpster, 2001; Goulao and Oliveira, 2008; Mercado *et al.*, 2011). Other cell wall proteins with no hydrolytic enzymatic activity, such as expansins, also have a role in softening (Brummell *et al.*, 1999). In general, the cell wall disassembly process responsible for softening involves the depolymerization of matrix glycans, the solubilization and depolymerization of pectins and the loss of neutral sugars from pectin-side chains (Brummell, 2006; Goulao and Oliveira, 2008). The extension of these changes greatly varies among different species (Mercado *et al.*, 2011). Recently, it has been suggested that the structural integrity of xyloglucan network performed by xyloglucosyltransferase /endohydrolase (XTH) could be important during fruit softening. This activity is generally higher during fruit expansion and then declines or remains constant during ripening (Goulao *et al*., 2007; Mercado *et al*., 2011). Miedes and Lorences (2009) suggested that *XTH* genes could be involved in the maintenance of cell wall structure rather than cell wall disassembly, and therefore, the decrease in *XTH* gene expression and activity could contribute to softening. Supporting this hypothesis, the

overexpression of *SlXTH1* gene in tomato reduced fruit softening (Miedes *et al*., 2010). In the other hand, although less studied than cell wall disassembly, cellular turgor also plays a role in fruit softening (Harker *et al.*, 1997). A loss of turgor pressure is generally observed during fruit ripening due to a regulated accumulation of apoplastic solutes (Wada *et al.*, 2009). Transpirational water loss through the cuticle could also be involved, especially in fruits with thick and well developed cuticles such as tomato (Saladié *et al.*, 2007; Lara *et al*., 2014). Cell turgor may also be influenced by cell wall modifications taking place during fruit softening (Thomas *et al.*, 2008), and it is therefore difficult to separate active turgor changes from those effects due to passive water loss and modification of cell wall mechanical properties.

Pectin is the most abundant polymer in the middle lamella regulating intercellular adhesion (Willats *et al.*, 2001), but primary fruit cell walls are also rich in polyuronides, accounting for up to 60% of cell wall mass in many fruits (Redgwell *et al.*, 1997*a*). Probably, pectins are the cell wall components that change most during fruit softening, but their role in fruit firmness and softening is considered somehow controversial. This could be due to the results obtained with tomato fruit which has been extensively used as a model species to study fruit ripening. Ripening of this fruit is characterized by a high increase in PG mRNA levels, protein and enzymatic activity which correlates with the rate of softening (Brummell and Harpster, 2001). However, the down-regulation of a PG gene to reach a residual gene expression of 1% when compared with wild type fruits did not reduce softening, although transgenic overripe fruits showed an improved storage life (Smith *et al.*, 1990; Kramer *et al.*, 1992; Brummell and Labavitich, 1997). Even more, although depolymerization of solubilized pectins was suppressed in transgenic tomatoes, the solubility of pectins remained at wild-type levels (Smith *et al.*, 1990). These early findings lead to the hypothesis that

PG-mediated pectin disassembly is neither necessary nor sufficient to induce fruit softening, especially at early stages of the process (Hadfield and Bennett, 1998). This hypothesis was later supported by studies performed in the tomato mutant *rin* showing an altered ripening behavior (Giovanoni *et al.*, 1989). However, more recent evidences in different species suggest an important role of pectin modifications in fruit softening. Thus, the down-regulation of a pectate lyase or a PG gene in strawberry significantly reduced fruit softening (Jiménez-Bermúdez *et al.*, 2002; Quesada *et al.*, 2009). Similarly, silencing of PG1 gene in apple, a crisp fruit with textural features completely different to strawberry, also diminished softening (Atkinson *et al.*, 2012).

Pectin is one the most complex natural plant biopolymers (Vincken *et al.*, 2003; Voragen *et al.*, 2009). This complexity makes polyuronides difficult to characterize and to infer their role in the cell wall when analyzed by conventional techniques, most of them relying on measuring the colligative properties and characteristics of a population of polysaccharides (Round *et al.*, 2001). Atomic force microscopy (AFM) allows the analysis of individual polymer chains and to study the degree of heterogeneity within a sample with minimal sample preparation (Morris *et al.*, 2010; Liu and Cheng, 2011). This technique has been used to determine the structure and functionality of polysaccharides from different sources, mainly focusing on aspects related to food characteristics (Kirby *et al.*, 1995*a*; Morris *et al.*, 2001). However, AFM has scarcely been used to study pectin modifications during fruit softening. The aim of this paper was to review the potential of AFM as a tool to gain insight into the pectin disassembly process during fruit ripening.

PECTIN DISASSEMBLY DURING FRUIT RIPENING

Traditional methodological approaches to study cell wall disassembly during ripening

involve the purification of cell wall and the isolation of different cell wall fractions based on their solubility on different solvents (Brett and Waldron, 1996). In this approach, pectins are extracted from cell wall material after sequential treatments with water or PAW (phenol:acetic acid:water); chelating agents such as trans-1,2-diaminocyclohexane-N,N,N'N'-tetraacetic acid (CDTA), solubilizing pectins ionically bound to the cell wall; and sodium carbonate, releasing pectins covalently bound to the wall by ester linkages (Brummell, 2006). Despite the arbitrary nature of this sequential pectin extraction procedure, it has been suggested that fractions represent different polymer moieties *in muro*. Thus, water extraction yields mainly pectins (water soluble pectins, WSP) freely soluble in the apoplast and already solubilized by processes occurred in vivo (Redgwell *et al.*, 1992); chelated soluble pectins (CSP) present in the CDTA fraction are enriched in homogalacturonan (HGA) from the middle lamella; and sodium carbonate soluble pectins (SSP) show characteristically high ratios of neutral sugars to uronic acid, suggesting enrichment in rhamnogalactorunan I (RG-I) from the primary wall (Brummell, 2006). Significant amounts of polyuronides, usually enriched in neutral sugars, still remain in the cell wall after this sequential fractionation (Redgwell *et al.*, 1997*b*; Brummell *et al.*, 2004).

Pectin solubilization is a common feature in fleshy fruit ripening. This process refers to an increase in the content of pectin loosely bound to the cell wall, mainly WSP but in some cases also chelated-soluble pectins, that is paralleled to a decrease in the amount of covalently bound pectins. It is thought that pectin solubilization occurs at the expense of polyuronides tightly bound to the wall (Wakabayashi, 2000; Brummell, 2006; Mercado *et al.*, 2011). Pectin solubilization varies greatly among species. This process is very evident in fruits such as avocado (Wakabayashi *et al.*, 2000), kiwifruit, tomato, persimmon (Redgwell *et al.*, 1997*a*), strawberry (Figueroa *et al.*, 2010), melon (Rose *et*

al., 1998) or peach (Brummell *et al.*, 2004), but, in general, it is less important in fruit with a crisp texture at ripening, such as apple, watermelon or nashi pear (Redgwell *et al.*, 1997*a*; Hiwasa *et al.*, 2004). Several processes have been proposed as responsible for pectin solubilization. The loss of arabinan and galactan side chains from RG-I could contribute to the solubilization because neutral chains might anchor pectins into the wall either through binding to matrix glycans or cellulose (Popper and Fry, 2005; Zykwinska *et al.*, 2005) or by physical entanglement with other wall polymers. Supporting this hypothesis, many fruits show a marked loss of neutral residues, mainly arabinose and galactose, during ripening (Gross and Sams, 1984; Redgwell *et al.*, 1997*b*). However, neutral sugar loss and pectin solubilization are not correlated in some fruits, e.g., plum shows an extensive depolymerization with no loss of arabinose or galactose, while apple and nashi pear show an extensive loss of galactose but a very slight pectin solubilization (Redgwell *et al.*, 1997*b*). According to Redgwell *et al.* (1997*b*) pectin solubilization and loss of galactose take place mostly in different cell wall polysaccharides. The loss of neutral sugars could also induce pectin solubilization indirectly, by increasing the wall porosity allowing the access of other hydrolase enzymes to their substrate. This hypothesis has been suggested by Smith *et al.* (2002) to explain the increase in firmness in transgenic tomato fruit with a β-Galactosidase gene silenced.

An alternative or complementary cause of solubilization would be the depolymerization of chelated and/or covalently bound pectins as result of the action of pectinase enzymes, such as polygalacturonase. Some fruits display a substantial loss of high molecular weight polymers coupled with an increase of intermediate and short pectins, e.g., avocado, tomato, peach, kiwifruit (Redgwell *et al.*, 1992; Huber and O´Donoghue, 1993; Redgwell *et al.*, 1997*a*; Brummell *et al.*, 2004). By contrast, other fruits show a low to moderate depolymerization of pectins, e.g. strawberry, blueberry,

melon, apple (Redgwell *et al.*, 1997*a*; Rose *et al.*, 1998; Vicente *et al.*, 2007). Although depolymerization is not as general as polyuronide solubilization, recent evidences obtained in fruits with crisp and soft texture when ripened support a key role of pectinases in softening. In strawberry, a soft fruit, Jiménez-Bermúdez *et al.* (2002) showed that the silencing of a pectate lyase, an enzyme that catalyzes the cleavage of glycosidic bonds of de-esterified pectins by a β-elimination reaction, in contrast to the hydrolytic mechanism of PG, resulted in fruits firmer than the control at the ripening stage, without affecting other fruit quality traits such as soluble solids, color or anthocyanin content. Cell wall analyses of these fruits indicated a lower depolymerization of chelated and sodium carbonate soluble pectins, as well as a lower degree of pectin solubilization (Santiago-Doménech *et al.*, 2008). More recently, Quesada *et al.* (2009) obtained strawberry plants with a PG gene down-regulated. These plants displayed a significant increase in fruit firmness at ripening, even higher than those of plants obtained with the silencing of the pectate lyase gene (García-Gago *et al.*, 2009). Cell wall modifications detected in these fruits were similar to those of the antisense pectate lyase plants, i.e. a 42% decrease in polyuronide solubilization concurrently with a slightly lower depolymerization of chelated and covalently bound pectins, a decreased cell wall swelling and an increase in cell to cell adhesion (Posé *et al.*, 2013). The silencing of a PG gene in apple, a fruit with a crisp texture, caused cell wall changes similar to those described for strawberry and also improved fruit firmness and textural characteristics (Atkinson *et al.*, 2012). This set of results challenge the previous notion that pectin depolymerization alone is not the determinant of softening, an idea mainly supported by the minor effect of PG silencing on tomato fruit firmness observed in earlier works (Haldfield and Bennett, 1998).

Progressive demethylesterification of HGA by pectin methyl esterase (PME)

action is common to the ripening of many fruits, creating large regions of negatively-charged side groups (Prasanna *et al.*, 2007; Goulao and Oliveira, 2008). In the absence of Ca^{2+}, this cell wall modification would contribute to the loosening of pectins by electrostatic repulsion (Brummell, 2006). However, Ca^{2+} concentration in the apoplast is high enough to allow cross-linking of unesterifed HGA chains by ionic interactions (Almeida and Huber, 1999). Furthermore, functional studies of PME genes in tomato (Tieman and Handa, 1994) and *Fragaria vesca* (Osorio *et al.*, 2008) failed to find an effect of this gene in fruit firmness. However, the degree of pectin esterification could be related to tissue integrity and cell adhesion. Thus, transgenic tomato fruits with the PME gene silenced showed a reduced shelf life as result of an almost complete loss of tissue integrity in senescent fruits (Tieman and Handa, 1994). An altered pattern of methyl-esterification has also been observed in the *Cnr* (*Colourless non-ripening*) tomato mutant, which fails to soften but displays a severe reduction in pericarp cell adhesion (Orfila *et al.*, 2002). Alternative hypotheses to explain the solubilization of pectins during fruit ripening are the synthesis of more freely soluble forms of pectin as the fruit ripens (Huber, 1984) or the degradation of RG-I backbone by rhamnogalacturonases (Molina-Hidalgo *et al.*, 2013). These last authors found that transient silencing of a gene encoding a rhamnogalacturonate lyase prevented the dissolution of the middle lamella during strawberry fruit ripening, suggesting a key role of RG-I in fruit softening.

In conclusion, the processes that lead to solubilization of polyuronides in the wall during fruit softening are diverse and recent evidences support a role for polyuronide depolymerization as one of the main mechanism involved, in spite of it was initially discarded as a possible cause. Altogether, the involvement of different mechanisms depending on the species could be probable. As suggested by Brummell

(2006), a better understanding of how HGA, RG-I and RG-II are interconnected to each other and to other polymers in the wall would help to explain this issue. The nano-structural characterization by AFM of the pectic chains present in these fractions and their structural modifications during ripening would shed light on how chains processing occurs during softening. The potential of this approach to provide a better knowledge of this process is discussed in the next sections.

AFM ANALYSIS OF FRUIT PECTINS

AFM fundamentals

Atomic force microscope belongs to a family of instruments known as scanning probe microscopes that generate images of the samples by "feeling" rather than "looking" the specimen, allowing higher magnification than light microscopy and comparable magnification to electronic microscopy but obtainable under the more natural conditions used for light microscopy (Morris *et al.*, 2010). In brief, a sharp tip is scanned relative to the sample surface and the changes in the magnitude of the force between tip and sample, are measured and used to produce a three dimensional image (profile) of the surface topography of the sample with subnanometer resolution. The sample is mounted in a liquid cell on top of a piezoelectric transducer controlling the motion of the sample in the three spatial dimensions at high resolution. The tip is positioned on a flexible cantilever allowing the tip to move up and down as it tracks across the sample. The cantilever deflection, and hence the displacement of the tip, is monitored using a laser beam focused onto the end of the cantilever and then, reflected off onto a four quadrant photodiode detector. As the tip moves in response to the sample topography the angle of the reflected laser beam changes and the movement of the reflected spot on the surface of the photodetector is recorded as an electrical potential difference (error signal). This

error signal can be used in a number of ways to generate a variety of images of the sample surface or of objects deposited onto this surface. A full description of this system and the different operation modes is described elsewhere (Kirby *et al.*, 1995*a*; Morris *et al.*, 2010). In addition to the molecular/sub-molecular resolution of this microscope for biological systems, AFM allows the visualization of samples with minimal preparation under natural or physiological conditions, in air or aqueous environments (Morris *et al.*, 2010; Liu and Cheng, 2011).

Each type of sample requires the selection of the appropriate imaging mode. Among the materials that can be used as solid phase, freshly cleaved mica is the most common because it is atomically flat, easy handling and cost-effective (Kirby *et al.,* 1995*a*). Then, polymers must be evenly spread over that surface in order to be visualized individually, by drop-deposition or by sprays. Two main methods are used for imaging polysaccharides (Kirby *et al.*, 1995*a*; Morris *et al.*, 2010). In the first case, polymers are imaged in the DC contact mode under alcohols with the AFM tip into direct contact with the sample. Usually, imaging is done under a liquid, propanol or butanol, which allows a greater precision in the control of the applied forces (Morris *et al.*, 2010). In this mode, as the probe is permanently in contact with the sample, high contrast images are obtained, although a shear force can be generated causing damages to the probe but also to the sample in case of being greatly soft. In the second method used to image polysaccharides, samples are imaged in the AC non contact mode under air (McIntire and Brandt, 1997). Briefly, in this mode the cantilever is oscillated at a constant frequency above the sample and the weak attractive forces between tip and sample are monitored. As the sample is being viewed from a greater effective distance, there is a loss of resolution compared to conventional AFM. When the same samples have been studied with both techniques, similar results have been obtained (Morris *et al.*,

2010). A variant of the non contact mode is known as tapping mode. In this case, during oscillation the probe contacts the surface of the sample intermittently at the lowest point, increasing the contrast of images from normal AC mode, reducing lateral forces during imaging and minimizing sample damaging (Morris *et al.*, 2010; Liu and Cheng, 2011). The three AFM techniques above described have been used to study nanostructure of pectins isolated from fruits (Table 1). A typical image of pectins isolated from strawberry fruit and visualized under butanol in contact mode is shown in Fig. 1. This image clearly shows the complexity of extracted pectin structures that might reflect the intricacy of the original pectin networks *in muro*.

Fruit pectin nanostructure

Table 1 summarizes the AFM available data about pectin fractions extracted from several fruits, including comparison between different developmental stages and cultivars with different textural properties. Early AFM studies focused on the analysis of pectins from unripe tomatoes. Round *et al.* (1997) analyzed pectin samples extracted with sodium carbonate. Images showed a mixed population of single polymers and aggregates. Interestingly, 20% of single polymers showed long branches with about 30% of these having more than one branch. Lengths of the main backbone ranged between 30 and 390 nm and size distribution fitted a log-normal curve. The range of length sizes for the branches was narrower, ranging from 30 to 170 nm. Apparently, the removal of acetyl and methyl groups during alkaline extraction to obtain the SSP fraction does not modify pectic chain nano-structure, since tomato pectins extracted with CDTA and visualized by AFM were similar to those present in the SSP samples. However, chain of the CDTA fraction were about 3 times longer than those extracted with sodium carbonate (Round *et al.*, 2001; Kirby *et al.*, 2008). Complementary analyses of neutral

sugar composition and linkage suggested that these branches do not correspond to neutral sugars (Round *et al.*, 2001), and it was postulated that the long branches observed in CSP, enriched in HGA, and SSP, enriched in RG-I, consist of polygalacturonic acid attached to the pectin backbone, with the neutral sugars present as short branches undetected by AFM (Round *et al.*, 2001). This result has been supported by subsequent AFM experiments on pectins from apple (Zareie *et al.*, 2003), peach (Yang *et al.*, 2009) and red ripe strawberry fruits (Posé *et al.*, 2012). In this last species, both CSP and SSP pectins showed a similar percentage of branched polymers, 8-9%, but SSP pectins showed smaller but more branches per backbone (Posé *et al.*, 2012). The lower size of SSP strawberry pectins correlated with the comparative profiles of both fraction obtained by size exclusion chromatography (Posé *et al*., 2012).

The polygalacturonic acid nature of the pectin branches observed by AFM has been strongly supported by experiments evaluating the effect of mild acid hydrolysis on SSP pectins from unripe tomato (Round *et al.*, 2010). This treatment releases different sugars residues present in polyuronides at different rates, with galactose and arabinose linkages the most labile and the galacturonic acid the most resistant (Thibault *et al.*, 1993). Round *et al.* (2010) observed that almost complete hydrolysis of galactose, arabinose and rhamnose has no significant effect on backbone and branch length distributions in individual pectins visualized by AFM. This result suggests that the observed single polymers were mainly formed by HGA and contain either no rhamnose or only small amounts located at the end of these chains. Besides isolated chains, complexes were also observed in these pectin samples, often possessing emerging strands with similar dimensions to isolated single chains. The size of the complexes observed in SSP samples by AFM decreased upon acid hydrolysis in parallel with the loss of neutral sugars. As the remnants of these complexes persisted after prolonged

hydrolysis, Round *et al.* (2010) suggested that they may contain RG-I linked to irreducible HGA. Therefore, AFM results offer a new image of sodium carbonate soluble pectin chains composition, consisting of linear and sparsely branched HGA and aggregated complexes containing RG-I, irreducible aggregates of HGA and HGA polysaccharide chains (Round *et al.*, 2010). The individual HGA chains observed either would be not linked to the RG-I or would be linked by bonds that are broken during cell wall fractionation. In this picture, neutral sugars would be coiled or aligned along and around the rhamnogalacturonan regions. Pectin aggregates of similar size and shape have been described in pectins from strawberry fruits as can be observed in Fig. 1.

In most AFM studies, pectin length varied in the range from 20 to 1000 nm, with pectin present in CSP in general longer than those observed in SSP (Table 1). However, pectin lengths several times higher than the range above described have been reported for some fruits, e.g., peach (Yang *et al.*, 2009), unripe jujube (Wang *et al.*, 2012). In SSP pectins from ripe strawberry fruit, Posé *et al.* (2012) also described the presence of large fibers within the background of individual molecules and aggregates, but these fibers disappeared when the samples were heated at 80ºC. Whether these large fibers represent novel supramolecular pectin structures, or whether they are artifacts formed during the extraction and/or deposition of the samples on the mica substrate, needs to be addressed. Besides pectin length, AFM allows the tridimensional measurement of pectin chains. Most reports indicate a height of the pectin chain in the range 0.5-2 nm. These measurements are in accordance with a helix structure of the chains with different aggregation status (Yang *et al.*, 2009), since the vertical height of single-stranded polysaccharides is about 0.5 nm (McIntire and Brant, 1999). Contrary to height measurements, there is great variation in pectin chain widths amongst the different reports. Yang *et al.* (2009) observed that widths of pectins from peaches varied between

20 to 100 nm, not observing significant differences either among the pectin fractions analyzed (WSP, CSP and SSP) or peach genotypes. By contrast, in strawberry fruit the width of SSP chains was smaller than those of WSP or CSP, ranging the values between 15 to 78 nm (Chen *et al.*, 2011). Xin *et al.* (2010) reported a mean width value of CSP pectin chains of 35 nm in unripe tomato fruit which decreased to 23 nm in turning fruit. Numerical regularities for the different pectin chain widths estimated in a sample have also been reported for some fruits. For example, Zhang *et al.* (2012) described that chain width of the WSP and CSP fractions from peach followed three basic units, 54, 72 and 91 nm, and the widths of other pectin chains could be obtained by the sum of these basic units. In the same fruit, Yang *et al.* (2005) observed four basic width units for WSP but these units were smaller than those reported by Zhang *et al.* (2012) (11.7, 15.6, 19.5 and 35.1 nm). A pattern of pectin chain width distribution has also been observed in SSP pectin chains from cherries with four basic units (37, 47, 55 and 61 nm) (Zhang *et al.*, 2008). These results could suggest a natural structural conformation of pectins formed by intertwists between these putative basic units. However, pectin width data should be considered with extreme caution and only used for qualitative comparison of objects within a particular sample. This is because the molecular width measured by AFM is subject to "probe broadening"; as the radius of the AFM tip is large relative to the diameter of the molecules being measured the image of the molecule being analyzed is convoluted with the tip profile and the measured dimension is considerably overestimated (Morris *et al.*, 2010). Kirby *et al.* (1995*b*) observed that thickness of individual strands of the bacterial polysaccharide acetan was 5 times greater than the value obtained when the measurements were performed in aggregated regions where the molecular chains had become aligned and the broadening effect was not present. McMaster *et al.* (1999), observed the width of a cylindrical object as about three times

greater than the actual value. Morris *et al.* (1997) and Fishman *et al.* (2007) described a geometrical correction to estimate the tip broadening effect. Probe broadening effects will vary with the actual radius of the tips used and can vary considerably from image to image. This might explain why chain width values reported are usually almost an order of magnitude higher than the observed pectin heights and, therefore the lack of correlation between pectin chain height and width, as well as the contradictory results obtained in different fruits and studies.

In general, nano-structural features of isolated pectins deduced from AFM images are in good agreement with data obtained using other approaches. Thibault *et al*. (1993), using high-performance size exclusion chromatography (HPSEC), reported that HGA pectins from different fruit sources hydrolyzed in 0.1M HCl contained approximately 72-100 galacturonic acid (GalA) residues. Similar degree of polymerization was found by Yapo *et al*. (2007) in HCl hydrolyzed citrus pectins using chromatographic techniques. According to Carpita and Gibeaut (1993), HGA contains up to 200 GalA units and are about 100 nm long. As above discussed, most AFM studies of isolated pectin chains reported a molecular length in the range 75-150 nm, which is in accordance with these data. The number of carbohydrate residues, as well as molecular weight, in individual pectins visualized by AFM can be estimated from contour length parameters considering that extended chains adopt a 3_1 helical structure with a pitch of 1.34 nm, as deduced by Walkinshaw and Arnott (1981) based on X-ray diffraction data. Using this approach, Round *et al*. (2010) found that minimum native size of linear chains in SSP pectins from unripe tomato could be around 320 residues, slightly higher than the polymerization degree of HGA purified by mild acid hydrolysis (Thibault *et al*., 1993; Yapo *et al*., 2007). However, it should be taking into account that pectin length can be greatly influenced by the ripening stage of the fruit source, as

discussed latter. As regard RG-I, the length of this polysaccharide is unknown (Carpita and McCann, 2000). McNeil *et al*. (1980) found that purified RG-I from sycamore cell walls treated with endopolygalacturonase had a MW of approximately 200 kDa, being the backbone formed by as many as 500 glycosyl residues. Interestingly, complexes found in AFM images of unripe tomato SSP pectins, which have been proposed to be composed mainly by RG-I, but also contains HGA chains, have a MW slightly higher, around 400 kDa (Round et al., 2010).

In summary, most nanostructural data of fruit pectins obtained by AFM analysis are in agreement with our previous knowledge on these polysaccharides, supporting the reliability of this approach to study pectin disassembly during fruit softening. The analysis of AFM published data differentiates two groups of reports, a first group describing pectin lengths below 1000 nm and widths between 10-50 nm, including data from tomato (Round *et al.*, 1997; 2010), strawberry (Posé *et al.*, 2012) and cherry (Zhang *et al.*, 2008; Lai *et al.*, 2013), and a second group which describe longer (>1000 nm) and wider (>50 nm) pectic chains, such as those observed in peach (Yang *et al.*, 2009), jujube (Wang *et al.*, 2012) and apricot (Chen *et al.*, 2013). Applying the width correction described by Morris *et al.* (1997), the first group of pectins would correspond mainly to individual pectin chains while the big fibers would be highly packed pectins of several hundreds of laterally arranged chains. If this high level of packaging exists or not *in muro* needs to be addressed in the future. Similarly, the physicochemical nature of micellar aggregates and its relationship with isolated pectin chains should be further investigated.

AFM analysis of pectins during fruit ripening and storage

Fruit texture is closely related to the structural integrity of fruit tissues and pectins play

a key role in cell to cell adhesion and cell wall stiffness. Several enzymes acting on pectins have been related to the changes that undergo cell walls during softening, such as PG, pectate lyase, PME, pectin acetylesterase, β-galactosidase, β-xylosidase, α-arabinofuranosidase (Brummell and Harpster, 2001; Goulao and Oliveira, 2008; Mercado *et al*., 2011). Although there are numerous reports about the biochemical changes in cell walls and pectins during fruit ripening and postharvest, few studies have been devoted to analyze these processes at the nano-structural scale. Zhang *et al.* (2008) used AFM to study chelate-soluble pectins isolated from two Chinese cherry cultivars with crisp and soft textures. Two ripening stages were also compared; commercial ripe fruit *vs* unripe fruit harvested 7 days before ripening. As expected, the firmer unripe fruits from both cultivars contained wider and longer chains than ripe fruits, as well as more polymers that were entangled together. However, comparison between cultivars did not support the same correlation, since firmness of the crisp cultivar was higher at both ripening stages, but its SSP fraction was richer in wider and shorter chains than the same fraction of soft fruits at both ripening stages. A similar study was performed by Xin *et al.* (2010) in CSP pectins from tomato. In this case, turning stage fruits contained wider chains than light-red fruits and linear single and short chains were more frequently observed in light-red tomatoes. Yang *et al.* (2009) analyzed three kinds of pectins (WSP, CSP and SSP) in two peach cultivars with contrasting texture, soft and crisp. The most significant difference between the two cultivars was the length of the SSP pectins, with the SSP chains of the crisp fruit longer than those of the soft cultivar, average lengths 249 vs. 57 nm, respectively. Additionally, a small number of CSP and SSP chains of the crisp genotype had branches whilst few or no branched polymers appeared in the soft fruit pectin fractions. These authors suggested that differences in texture in peach could be mainly related to the neutral-sugar rich pectin fraction from

the primary cell wall. In Chinese jujube fruits, pectin length also decreased during ripening (Wang *et al.*, 2012).

Representative topographical AFM images of CSP pectins from strawberry fruit at two ripening stages are shown in Fig. 1 to illustrate the pectin modifications that frequently occur during fruit ripening. Qualitative analysis of these images showed that CSP samples from unripe fruits (Fig. 1-A) were enriched in long chains while shorter chains were more frequently observed in red fruits (Fig. 1-B). Branched polymers (Fig. 1-F) could be observed in both samples, unripe and ripe, but the frequency of branching decreased in ripe samples. Some aggregates with emergent polymer strands could also be observed in these samples (Fig. 1-E).

The nano-structural changes in pectins during fruit storage have been analyzed in a few numbers of species. In peach fruit stored at different temperatures (2, 8 and 15ºC) Zhang *et al.* (2010) observed an increase in the content of WSP and CSP and a decrease in SSP during storage in parallel to a decrease in fruit firmness, with this higher at higher temperature. However, fruit firmness was only correlated with the content of SSP pectin. An AFM study of this fraction showed that most SSP pectins formed large aggregates in fresh fruits that were reduced during the storage period, along with the rise of the storage temperature. Furthermore, the length and width of the pectin chains were reduced with storage time and higher temperatures. A similar result was observed when WSP and CSP were analyzed, although CSP pectins fruits at harvest were visualized mainly as single linear chains with a small number of aggregates (Zhang *et al.*, 2012). The beneficial effects of controlled atmospheres, 2% O_2 and 5-10% CO_2, in the quality of peach stored at low temperature have also been related to a lower degradation of pectins at the nanostructural level (Yang *et al.*, 2005; Yang *et al.*, 2006*a*, 2006*b*). Interestingly, a decrease in the number of branched polymers was observed with

storage time and it was concomitant to a reduction of pectin size and number of aggregates (Yang *et al.*, 2005; Yang *et al.*, 2006*a*, 2006*b*). In CSP pectins from apricots stored at 0ºC, Liu *et al.* (2009) also observed a decrease on the percentage of branched polymers with the storage time. Furthermore, the frequency of short CSP chains increased with time and the application of $CaCl_2$, a treatment that extends the postharvest life, supposedly due to the formation of calcium bridges between HGA chains, partially reduced the degradation of pectins (Liu *et al.*, 2009). Length of WSP and SSP from strawberries decreased a 30-39% during the storage of the fruit at 4ºC for 15 days (Chen *et al.*, 2011). As previously observed in apricot, $CaCl_2$ treatments partially reduced the depolymerization of strawberry SSP polyuronides (Chen *et al.*, 2011).

Besides the study of individual pectin polymers, AFM provides a useful means to study their aggregation and the effect of factors affecting the formation of gels, e.g. acid-induced and calcium-induced gelation, pectin concentration (Fishman *et al*., 2007; Morris *et al*., 2010; Morris *et al*., 2011). Most of these studies have been performed with fruit pectins extracted with chelating agents but they have not been related to the process of fruit softening. The structural information derived from gelation studies could be useful to understand the self-assembly process in the middle lamella (Morris *et al*., 2011), a region that is substantially modified during fruit ripening. AFM could therefore provide a new tool to unravel the role of pectin aggregation in the middle lamella dissolution process during fruit ripening.

CONCLUSIONS

Summarizing, the nano-structural characterization of pectins by AFM in fleshy fruits revealed significant modifications of the pectic chains and aggregates present in the

pectin samples during fruit ripening and postharvest storage. In general, these changes involve a decrease in the number of pectin aggregates and a reduction in the length of individual pectin chains and in the width of highly packed pectins, especially those extracted with sodium carbonate, supposedly located within the primary cell wall. Although additional work is needed to identify the physicochemical bases of the structures visualized by AFM, this technique could be a powerful tool to gain insight into the role of pectin disassembly mechanisms during fruit softening. At present, it has already provided consistent evidences of differences in pectic chains and aggregates correlated with ripening stages and storage treatments.

FUNDING

This work was supported by the Ministerio de Educación y Ciencia of Spain and Feder EU Funds [grant reference AGL2011-24814]. CP was supported with a FPI fellowship from the Spanish Government [grant reference BES-2009-027985]. The research at IFR was supported through the BBSRC core grant to the Institute.

LITERATURE CITED

Almeida DPF, Huber DJ. 1999. Apoplastic pH and inorganic ion levels in tomato fruit: a potential means for regulation of cell wall metabolism during ripening. *Physiologia Plantarum* **105:** 506-512.

Atkinson RG, Sutherland PW, Johnston SL, Gunaseelan K, Hallett IC, Mitra D, Brummell DA, Schröder R, Johnston JW, Schaffer RJ. 2012. Down-regulation of *POLYGALACTURONASE1* alters firmness, tensile strength and water loss in apple (*Malus x domestica*) fruit. *BMC Plant Biology* **12:** 129-142.

Bapat VA, Trivedi PK, Ghosh A, Sane VA, Ganapathi TR, Nath P. 2010. Ripening of

fleshy fruit: molecular insight and the role of ethylene. *Biotechnology Advances* **28**: 94-107.

Bourne MC. 1979. Texture of temperate fruits. *Journal of Texture Studies* **10**: 25-44.

Brett C, Waldron K. 1996. Physiology and Biochemistry of Plant Cell Walls. Chapman & Hall.

Brummell DA. 2006. Cell wall disassembly in ripening fruit. *Functional Plant Biology* **33:** 103-119.

Brummell DA, Harpster MH. 2001. Cell wall metabolism in fruit softening and quality and its manipulation in transgenic plants. *Plant Molecular Biology* **47**: 311-340.

Brummell DA, Labavitch JM. 1997. Effect of antisense suppression of endopolygalacturonase activity on polyuronide molecular weight in ripening tomato fruit and in fruit homogenates. *Plant Physiology* **115:** 717-725.

Brummell DA, Harpster MH, Civello PM, Palys JM, Bennett AB, Dunsmuir P. 1999. Modification of expansin protein abundance in tomato fruit alters softening and cell wall polymer metabolism during ripening. *Plant Cell* **11**: 2203-2216.

Brummell DA, Del Cin V, Crisosto CH, Labavitch JM. 2004. Cell wall metabolism during maturation, ripening and senescence of peach fruit. *Journal of Experimental Botany* **55**: 2029-2039.

Carpita N, Gibeaut DM. 1993. Structural models of primary cell walls in flowering plants: consistency of molecular structure with the physical properties of the walls during growth. *The Plant Journal*, **3:** 1-30.

Carpita N, McCann M. 2000. The cell wall. In: Buchanan B, Gruissem W, Jones R, eds. *Biochemistry and Molecular Biology of Plants*. American Society of Plant Physiologist, 52-108.

Chen F, Liu H, Yang H, Lai S, Cheng X, Xin Y, Yang B, Hou H, Yao Y, Zhang S, Bu G, Deng Y. 2011. Quality attributes and cell wall properties of strawberries (*Fragaria annanassa* Duch.) under calcium chloride treatment. *Food Chemistry* **126:** 450-459.

Chen Y, Chen F, Lai S , Yang H, Liu H , Liu K, Bu G, Deng Y. 2013. In vitro study of the interaction between pectinase and chelate-soluble pectin in postharvest apricot fruits. *European Food Research and Technology* **217:** 1438-*2377*

Figueroa CR, Rosli HG, Civello PM, Martínez GA, Herrera R, Moya-León MA. 2010. Changes in cell wall polysaccharides and cell wall degrading enzymes during ripening of *Fragaria chiloensis* and *Fragaria* × *ananassa* fruits. *Scientia Horticulturae*, **124:** 454-462.

Fishman ML, Cooke PH, Chau HK, Coffin DR, Hotchkiss AT. 2007. Global structures of high methoxyl pectin from solution and in gels. *Bio-macromolecules* **8**: 573–578.

Gapper NE, McQuinn RP, Giovannoni JJ. 2013. Molecular and genetic regulation of fruit ripening. *Plant Molecular Biology* **82:** 575-591.

García-Gago JA, López-Aranda JM, Muñoz-Blanco J, Toro FJ, Quesada MA, Pliego-Alfaro F, Mercado JA. 2009. Postharvest behaviour of transgenic strawberry with polygalacturonase or pectate lyase genes silenced. *Acta Horticulturae* **842:** 573-576.

Giovannoni JJ, DellaPenna D, Bennett AB, Fischer RL. 1989. Expression of a chimeric polygalacturonase gene in transgenic rin (ripening inhibitor) tomato fruit results in polyuronide degradation but not fruit softening. *Plant Cell* **1:** 53-63.

Goulao LF, Oliveira CM. 2008. Cell wall modification during fruit ripening: when a fruit is not the fruit. *Trends in Food Science & Technology* **19**: 4-25.

Gross KC, Sams CE. 1984. Changes in cell wall neutral sugar composition during fruit ripening: a species survey. *Phytochemistry* **23:** 2457-2461.

Hadfield KA, Bennett AB. 1998. Polygalacturonases: many genes in search of a function. *Plant Physiology* **117:** 337-343.

Harker FR, Redgwell RJ, Hallet IC, Murray SH. 1997. Texture of fresh fruit. *Horticultural Review* **20:** 121-224.

Hiwasa K, Nakano R, Hashimoto A, Matsuzaki M, Murayama H, Inaba A, Kubo Y. 2004. European, chinese and japanese pear fruits exhibit differential softening characteristics during ripening. *Journal of Experimental Botany* **55:** 2281-2290.

Huber DJ. 1984. Strawberry fruit softening - the potential roles of polyuronides and hemicelluloses. *Journal of Food Science* **49:** 1310-1315.

Huber DJ, O´Donoghue EM. 1993. Polyuronides in avocado (*Persea americana*) and tomato (*Lycopersicon esculentum*) fruits exhibit markedly different patterns of molecular weight downshifts during ripening. *Plant Physiology* **102**: 473-480.

Jiménez-Bermúdez S, Redondo-Nevado J, Muñoz-Blanco J, Caballero JL, López-Aranda JM, Valpuesta V, Pliego-Alfaro F, Quesada MA, Mercado JA. 2002. Manipulation of strawberry fruit softening by antisense expression of a pectate lyase gene. *Plant Physiology* **128:** 751-759.

Kirby AR, Gunning AP, Morris VJ, Ridout MJ. 1995a. Atomic force microscopy in food research: a new technique comes of age. *Trends in Food Science and Technology* **6:** 359-365.

Kirby AR, Gunning AP, Morris VJ, Ridout MJ. 1995b. Observation of the helical structure of the bacterial polysaccharide acetan by atomic force microscopy. *Biophysical Journal* **68:** 360-363.

Kirby AR, MacDougall AJ, Morris VJ. 2008. Atomic force microscopy of tomato and

sugar beet pectin molecules. *Carbohydrate Polymers* **71:** 640-647.

Kramer M, Sanders R, Bolkan H, Waters C, Sheehy RE, Hiatt WR. 1992. Postharvest evaluation of transgenic tomatoes with reduced levels of polygalacturonase: processing, firmness and disease resistance. *Postharvest Biology and Technology* **1:** 241-255.

Lai S, Chen F, Zhang L, Yang H, Deng Y, Yang B. 2013. Nanostructural difference of water-soluble pectin and chelate-soluble pectin among ripening stages and cultivars of Chinese cherry. *Natural Product Research: Formerly Natural Product Letters*, **27**:4-5, 379-385.

Lara I, Belge B, Goulao LF. 2014. The fruit cuticle as a modulator of postharvest quality. *Postharvest Biology and Technology* **87:** 103-112.

Liu D, Cheng F. 2011. Advances in research on structural characterisation of agricultural products using atomic force microscopy. *Journal of the Science of Food and Agriculture* **91:** 783-788.

Liu H, Chen F, Yang H, Yao Y, Gong X, Xin Y, Ding C. 2009. Effect of calcium treatment on nanostructure of chelate-soluble pectin and physicochemical and textural properties of apricot fruits. *Food Research International* **42:** 1131-1140.

McIntire, TM, Brant DA. 1999. Imaging of carrageenan macrocycles and amylose using noncontact atomic force microscopy. *International Journal of Biological Macromolecules* **26:** 303-310.

McIntire TM, Brant DA. 1997. Imaging of individual biopolymers and supramolecular assemblies using noncontact atomic force microscopy. *Biopolymers* **42:** 133-146.

McMaster TJ, Miles MJ, Kasarda DD, Shewry PR, Tatham AS. 1999. Atomic force microscopy of A-gliadin fibrils and in situ degradation. *Journal of Cereal Science* **31:** 281-286.

McNeil M, Darvill AG, Albersheim P. 1980. Structure of plant cell walls. X. Rhamnogalacturonan I, a structurally complex pectic polysaccharide in the walls of suspension-cultured sycamore cells. *Plant Physiology* **66:** 1128-1134.

Mercado JA, Pliego-Alfaro F, Quesada MA. 2011. Fruit shelf life and potential for its genetic improvement. In: Jenks MA, Bebeli PJ, eds. *Breeding for Fruit Quality.* Oxford: John Wiley & Sons, Inc., 81-104.

Miedes E, Lorences EP. 2009. Xyloglucan endotransglucosylase/hydrolases (XTHs) during tomato fruit growth and ripening. *Journal of Plant Physiology* **166**: 489-498.

Miedes E, Herbers K, Sonnewald U, Lorences. 2010. Overexpression of a cell wall enzyme reduces xyloglucan depolymerization and softening of transgenic tomato fruits. *Journal of Agricultural Food Chemistry* **58**: 5708-2713.

Molina-Hidalgo FJ, Franco AR, Villatoro C, Medina-Puche L, Mercado JA, Hidalgo MA, Monfort A, Caballero JL, Muñoz-Blanco J, Blanco-Portales R. **2013.** The strawberry (*Fragaria* × *ananassa*) fruit-specific *rhamnogalacturonate lyase 1* (*FaRGLyase1*) gene encodes an enzyme involved in the degradation of cell-wall middle lamellae. *Journal of Experimental Botany* **64:** 1471-1483.

Morris VJ, Gunning AP, Kirby AR, Round A, Waldron K. **1997**. Atomic force microscopy of plant cell wall, plant cell wall polysaccharides and gels. *International Journal of Biological Macromolecules* **21**: 61-66.

Morris VJ, Mackie AR, Wilde PJ, Kirby AR, Mills EC, Gunning AP. 2001. Atomic force microscopy as a tool for interpreting the rheology of food biopolymers at the molecular level. *LW T-Food Science and Technology* **34:** 3-10.

Morris VJ, Kirby AR, Gunning AP. 2010. Atomic Force Microscopy for Biologists. Imperial College Press, London.

Morris VJ, Gromer A, Kirby AR, Bongaerts RJM, Gunning AP. 2011. Using AFM

and force spectroscopy to determine pectin structure and (bio) functionality. *Food Hydrocolloids* **25:** 230-237.

Orfila C, Huisman MMH, Willats WGT, van Alebeek GJWM, Schols HA, Seymour GB, Knox JP. 2002. Altered cell wall disassembly during ripening of *Cnr* tomato fruit: implications for cell adhesion and fruit softening. *Planta* **215:** 440-447.

Osorio S, Castillejo C, Quesada MA, Medina-Escobar N, Brownsey GJ, Suau R, Heredia A, Botella MA, Valpuesta V. 2008. Partial demethylation of oligogalacturonides by pectin methyl esterase 1 is required for eliciting defence responses in wild strawberry (*Fragaria vesca*). *Plant Journal* **54:** 43–55.

Popper ZA, Fry SC. 2005. Widespread occurrence of a covalent linkage between xyloglucan and acidic polysaccharides in suspension-cultured angiosperm cells. *Annals of Botany* **96:** 91-99.

Posé S, Kirby AR, Mercado JA, Morris VJ, Quesada MA. 2012. Structural characterization of cell wall pectin fractions in ripe strawberry fruits using AFM. *Carbohydrate Polymers* **88:** 882-890.

Posé S, Paniagua C, Cifuentes M, Blanco-Portales R, Quesada MA, Mercado JA. 2013. Insights into the effects of polygalacturonase *FaPG1* gene silencing on pectin matrix disassembly, enhanced tissue integrity, and firmness in ripe strawberry fruits. *Journal of Experimental Botany* **64:** 3803-3815.

Prasanna V, Prabha TN, Tharanathan RN. 2007. Fruit ripening phenomena – An overview. *Critical Reviews in Food Science and Nutrition* **47:** 1-19.

Quesada MA, Blanco-Portales R, Posé S, García-Gago JA, Jiménez-Bermúdez S, Muñoz-Serrano A, Caballero JL, Pliego-Alfaro F, Mercado JA, Muñoz-Blanco J. 2009. Antisense down-regulation of the *FaPG1* gene reveals an unexpected

central role for polygalacturonase in strawberry fruit softening. *Plant Physiology* **150:** 1022-1032.

Redgwell RJ, Melton LD, Brasch DJ. 1992. Cell wall dissolution in ripening kiwifruit (*Actinidia deliciosa*): solubilisation of the pectic polymers. *Plant Physiology* **98**: 71-81.

Redgwell RJ, Macrae E, Hallett I, Fischer M, Perry J, Harker R. 1997a. In vivo and in vitro swelling of cell walls during fruit ripening. *Planta* **203:** 162-173.

Redgwell RJ, Fischer M, Kendall E, MacRae EA Perry J, Harker R. 1997b. Galactose loss and fruit ripening: high-molecular-weight arabinogalactans in the pectic polysaccharides of fruit cell walls. *Planta* **203:** 174-181.

Rose JKC, Hadfield KA, Labavitch JM, Bennett AB. 1998. Temporal sequence of cell wall disassembly in rapidly ripening melon fruit. *Plant Physiology* **117:** 345-361.

Rosli HG, Civello PM, Martinez GA. 2004. Changes in cell wall composition of three *Fragaria x ananassa* cultivars with different softening rate during ripening. *Plant Physiology and Biochemestry* **42:** 823-831.

Round AN, MacDougall AJ, Ring SG, Morris VJ. 1997. Unexpected branching in pectin observed by atomic force microscopy. *Carbohydrate Research* **303**: 251-253

Round AN, Rigby NM, MacDougall AJ, Ring SG, Morris VJ. 2001. Investigating the nature of branching in pectin by atomic force microscopy and carbohydrate analysis. *Carbohydrate Research* **331**: 337-342.

Round AN, Rigby NM, MacDougall AJ, Morris VJ. 2010. A new view of pectin structure revealed by acid hydrolysis and atomic force microscopy. *Carbohydrate Research* **345:** 487-497.

Saladié M, Matas AJ, Isaacson T, Jenks MA, Goodwin SM, Niklas KJ, Xiaolion R,

Labavitch JM, Shackel KA, Fernie AR, Lytovchenko A, O'Neill MA, Watkins CB, Rose JKC. 2007. A reevaluation of the key factors that influence tomato fruit softening and integrity. *Plant Physiology* **144:** 1012-1028.

Santiago-Doménech N, Jiménez-Bermúdez S, Matas AJ, Rose JKC, Muñoz-Blanco J, Mercado JA, Quesada MA. 2008. Antisense inhibition of a pectate lyase gene supports a role for pectin depolymerization in strawberry fruit softening. *Journal of Experimental Botany* **59:** 2769-2779.

Smith CJS, Watson CF, Morris PC, Bird CR, Seymour GB, Gray JE, Arnold C, Tucker GA, Schuch W, Harding S, Grierson D. 1990. Inheritance and effect on ripening of antisense polygalacturonase genes in transgenic tomatoes. *Plant Molecular Biology* **14:** 369-379.

Smith DL, Abbott JA, Gross KC. 2002. Down-regulation of tomato β-galactosidase 4 results in decreased fruit softening. *Plant Physiology* **129:** 1755-1762.

Thibault J-F, Renard CMGC, Axelos MAV, Roger P, Crépeau M-J. 1993. Studies of the length of homogalacturonic regions in pectins by acid hydrolysis. *Carbohydrate Research* **238:** 271-286.

Thomas TR, Shackel KA, Matthews MA. 2008. Mesocarp cell turgor in *Vitis vinifera* L. berries throughout development and its relation to firmness, growth, and the onset of ripening. *Planta* **228:** 1067-1076.

Tieman DM, Handa AK. 1994. Reduction in pectin methylesterase activity modifies tissue integrity and cation levels in ripening tomato (*Lycopersicom esculentum* Mill.) fruits. *Plant Physiology* **106:** 429-436.

Toivonen PM, Brummell DA. 2008. Biochemical bases of appearance and texture changes in fresh-cut fruit and vegetables. *Postharvest Biology and Technology* **48**: 1-14.

Vicente AR, Ortugno C, Powell ALT, Greve LC, Labavitch JM. 2007. Temporal sequence of cell wall disassembly events in developing fruits. 1. Analysis of raspberry (*Rubus idaeus*). *Journal of Agricultural and Food Chemistry* **55:** 4119-4124.

Vincken JP, Schols HA, Oomen RJFJ, McCann MC, Ulvskov P, Voragen AGJ, Visser RGF. 2003. If homogalacturonan were a side chain of rhamnogalacturonan I. Implications for cell wall architecture. *Plant Physiology* **132**: 1781-1789.

Voragen A, Coenen G, Verhoef R, Schols H. 2009. Pectin, a versatile polysaccharide present in plant cell walls. *Structural Chemistry* **20**: 263-275.

Wada H, Matthews MA, Shackel KA. 2009. Seasonal pattern of apoplastic solute accumulation and loss of cell turgor during ripening of *Vitis vinifera* fruit under field conditions. *Journal of Experimental Botany* **60:** 1773-1781.

Wakabayashi K. 2000. Changes in cell wall polysaccharides during fruit ripening. *Journal of Plant Research* **113:** 231-237.

Wakabayashi K, Chun J-P, Huber DJ. 2000. Extensive solubilization and depolymerization of cell wall polysaccharides during avocado (*Persea americana*) ripening involves concerted action of polygalacturonase and pectinmethylesterase. *Physiologia Plantarum* **108**: 345-352.

Wang H, Chen F, Yang H, Chen Y, Zhang L, An H. 2012. Effects of ripening stage and cultivar on physicochemical properties and pectin nanostructure of jujubes. *Carbohydrate Polymers* **89:** 1180-1188.

Willats WG, McCartney L, Mackie W, Knox JP. 2001. Pectin: cell biology and prospects for functional analysis. *Plant Molecular Biology* **47:** 9-27.

Xin Y, Chen F, Yang H, Zhang P, Deng Y, Yang B. 2010. Morphology, profile and role of chelate-soluble pectin on tomato properties during ripening. *Food Chemistry* **121:**

372-380.

Yang H, An H, Feng G, Li Y, Lai S. 2005. Atomic force microscopy of the water-soluble pectin of peaches during storage. *European Food Research and Technology* **220:** 587-591.

Yang H, Lai S, An H, Li Y. 2006a. Atomic force microscopy study of the ultrastructural changes of chelate-soluble pectin in peaches under controlled atmosphere storage. *Postharvest Biology and Technology* **39:** 75-83.

Yang H-S, Feng G-P, An H-J, Li Y-F. 2006b. Microstructure changes of sodium carbonate-soluble pectin of peach by AFM during controlled atmosphere storage. *Food Chemistry* **94:** 179-192.

Yang H, Chen F, An H, Lai S. **2009.** Comparative studies on nanostructures of three kinds of pectins in two peach cultivars using atomic force microscopy. *Postharvest Biology and Technology* **51** 391-398.

Yapo BM, Lerouge P, Thibault J-F, Ralet M-C. 2007. Pectins from citrus peel cell walls contain homogalacturonans homogeneous with respect to molar mass, rhamnogalacturonan I and rhamnogalacturonan II. *Carbohydrate Polymers*, **69:** 426-435.

Zareie MH, Gokmen V, Javadipour I. 2003. Investigating network, branching, gelation and enzymatic degradation in pectin by atomic force microscopy. *Journal of Food Science and Technology* **40:** 169-172.

Zhang L, Chen F, An H, Yang H, Sun X, Guo X, Li L. 2008. Physicochemical properties, firmness, and nanostructures of sodium carbonate-soluble pectin of 2 chinese cherry cultivars at 2 ripening stages. *Journal of Food Science* **73:** N17-N22.

Zhang L, Chen F, Yang H, Sun X, Liu H, Gong X, Jiang C, Ding C. 2010. Changes in firmness, pectin content and nanostructure of two crisp peach cultivars after

storage. *LWT-Food Science and Technology* **43:** 26-32.

Zhang L, Chen F, Yang H, Ye X, Sun X, Liu D, Yang B, An H, Deng Y. 2012. Effects of temperature and cultivar on nanostructural changes of water-soluble and chelate-soluble pectin in peaches. *Carbohydrate Polymers* **87:** 816-821.

Zykwinska AW, Ralet MCJ, Garnier CD, Thibault JFJ. 2005. Evidence for *in vitro* binding of pectin side chains to cellulose. *Plant Physiology* **139:** 397–407.

Table 1: A summary of AFM nano-structural characterization of pectins isolated from different fleshy fruit. ND= not described; DC= Direct contact; NC= non contact; TM= Tapping mode. WSP, CSP and SSP correspond to water-, chelated- and sodium carbonate- solubilized pectins, respectively.

Fruit	**Cultivar**	**Stage**	**Pectin fraction**	**Pectin length (nm)**	**Pectin width* (nm)**	**Image condition**	**Reference**
Apricot (*Prunus armeniaca* L.)	Jinhong	ripe	CSP	500-3000	23-234	Air; TP	Chen *et al.* (2013)
Cherry (*Prunus pseudocerasus* L.)	Caode Bende	unripe	WSP	ND	76-176	Air; DC	Lai *et al.* (2013)
			CSP	ND	37-61		
			SSP	448-749	37-140		Zhang *et al.* (2008)
		ripe	WSP	ND	37-82		Lai *et al.* (2013)
			CSP	ND	17-55		
			SSP	123-749	37-140		Zhang *et al.* (2008)
Jujube (*Zizyphus jujuba*)	Huanghua Zhanhua	unripe	CSP	500, >3000	23-98	Air; TM	Wang *et al.* (2012)
			SSP	500, >3000	35-156		
		ripe	CSP	□500, >3000	16-78		
			SSP	□500, 2500	16-78		
Peach (*Prunus persica* L. Batsch.)	Jinxiu Milu	ripe	WSP	300-4200	20-100	Air; TM	Yang *et al.* (2006*a*,*b*; 2009)

			CSP	100-3000	ND		
			SSP	20-900	35-70		
	Cangfangzaosheng Songsenzaosheng		WSP	ND	91-217	Air; NC	Zhang et al (2012)
			CSP	ND	91-181		
Strawberry (*Fragaria* x *annanassa* Duch.)	Chandler	ripe	CSP	20-500	ND	Butanol; DC	Posé *et al.* (2012)
			SSP	20-320	ND		
	Shijixiang		WSP	88-3043	23-78	Air; TM	Chen *et al.* (2011)
			CSP	ND	23-78		
			SSP	87-1152	23-59		
Tomato (*Lycopersicon esculentum* Mill.)	Rutger	unripe	CSP	40-560	ND	Butanol; DC	Kirby *et al.* (2008)
			SSP	20-400	ND	Butanol; DC	Round *et al.* (2010)
	Dongsheng Geruisi	turning	CSP	ND	19-117	Air; TM	Xin *et al.* (2010)
		ripe	CSP	ND	15-117		

*Width data correspond to non-corrected data and might be overestimated due to the probe broadening effect. See text for details.

Figure legends

Fig. 1: AFM topographical images representative of strawberry CSP pectins at unripe (A) and ripe (B) developmental stages, drop deposited onto mica and visualized by direct contact mode under butanol. Inlets (C-F) show zoomed areas from the A and B images showing examples of linear chains (C,D), multichain aggregates (E) and branched chains (F). (G) is equivalent to zoomed image D, and (H) is equivalent to zoomed image E showing the topographical details for linear chains and aggregates in 3D. Scale bars: for A and B are 250 nm; for C-F are 75 nm.

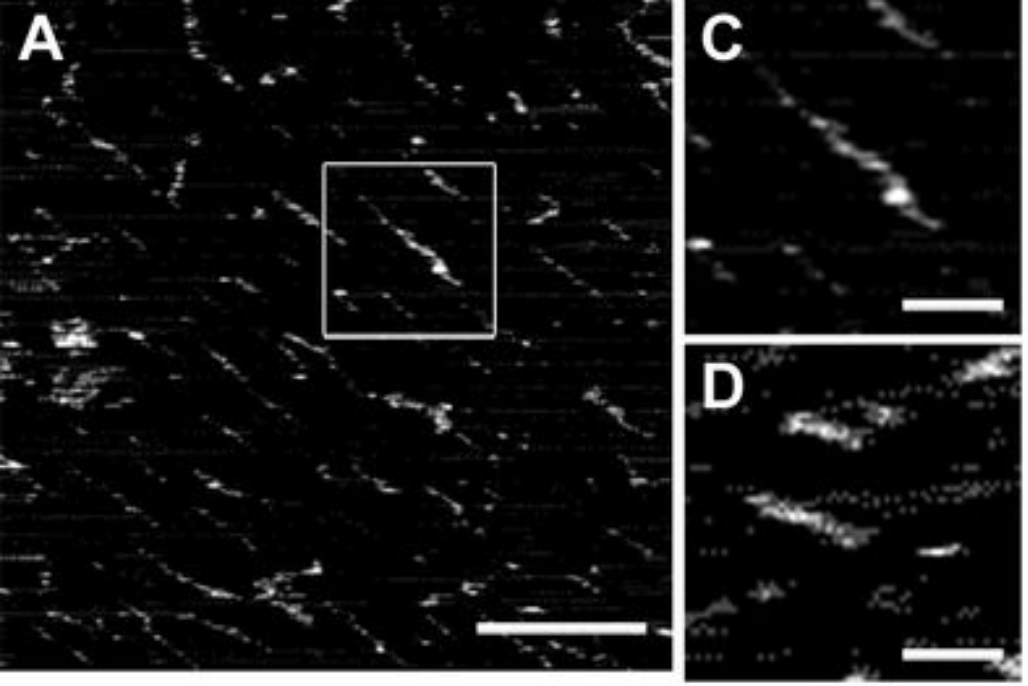
A

C

D

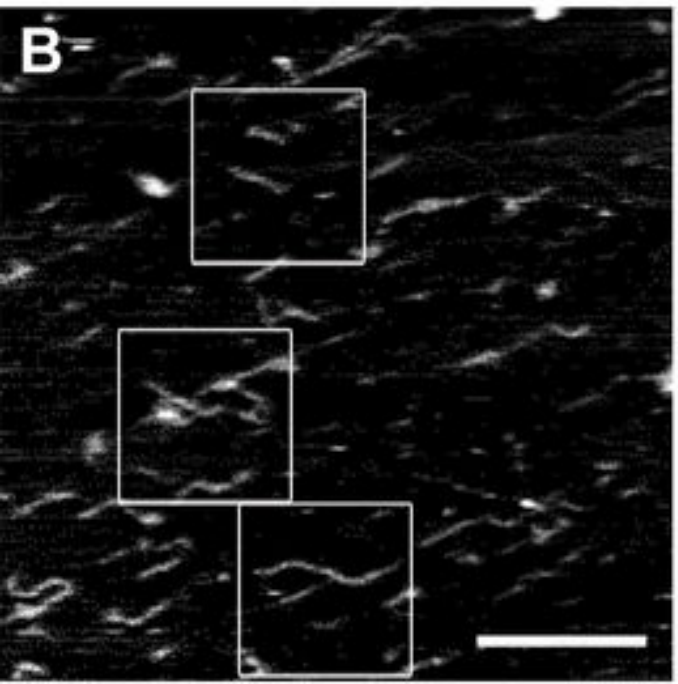
B

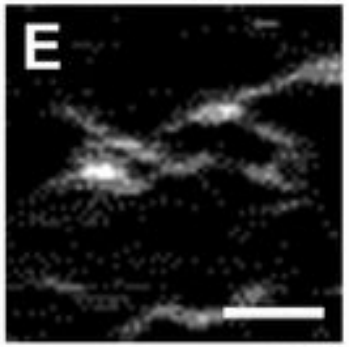
E

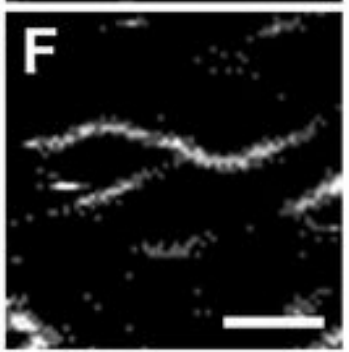
F

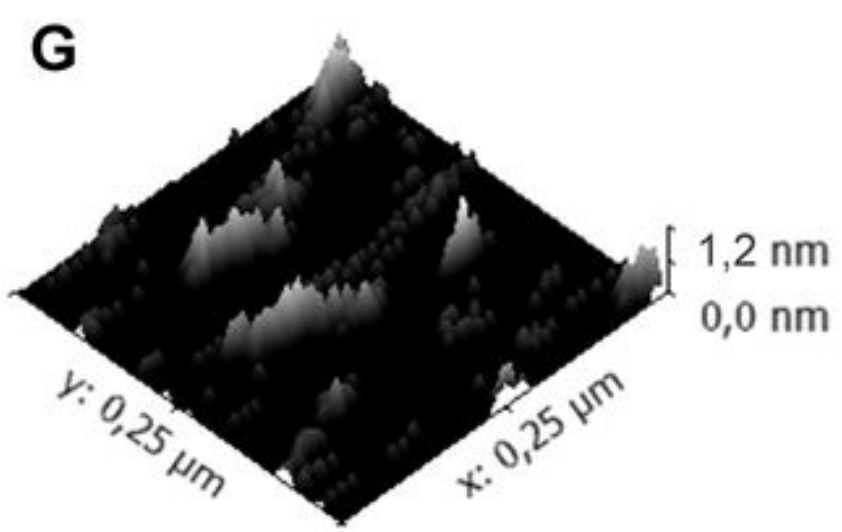
G
1,2 nm
0,0 nm
y: 0,25 µm
x: 0,25 µm

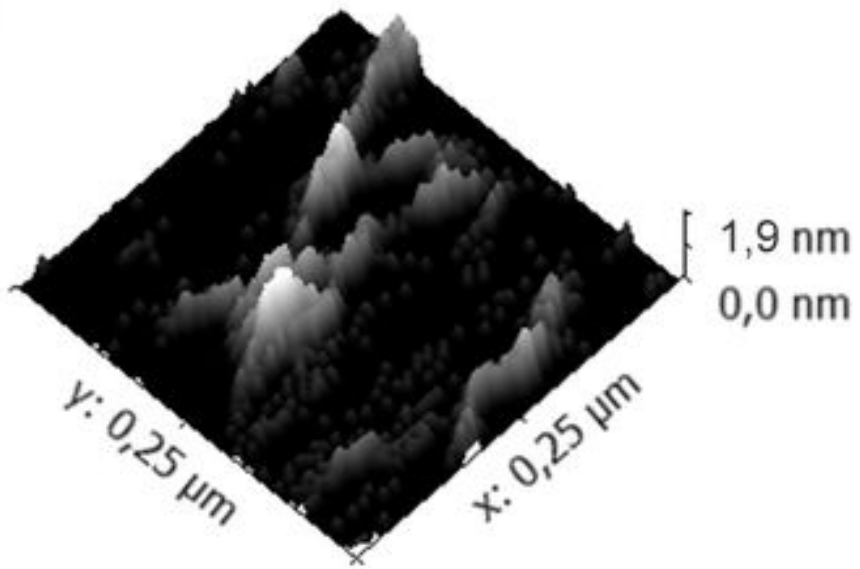
H
1,9 nm
0,0 nm
y: 0,25 µm
x: 0,25 µm